for 4 h. After bulb-to-bulb distillation, most of the ether was distilled off under atmospheric pressure. The residue afforded 1,1-dimethyl-4-methylene-1-silacyclohexa-2,5-diene (**24**; 6.5 mg, 0.048 mmol, 5.1%) by means of preparative GLC: oil; $^1$H NMR ($CDCl_3$) $\delta$ 0.12 (s, 6 H, SiMe), 5.27 (s, 2 H, $=CH_2$), 6.05 (d, 2 H, $J_{2,3} = J_{5,6} = 14.5$ Hz, H-2,6), 7.03 (d, 2 H, $J_{2,3} = J_{5,6} = 14.5$ Hz, H-3,5); IR (neat, cm$^{-1}$) 2980, 2950, 1615, 1550, 1245, 895, 840, 805, 765, 710; MS $m/z$ (%) 136 ($M^+$, 17), 121 (100), 95 (14), 69 (12); high-resolution MS found 136.0702, calcd for $C_8H_{12}Si$ 136.0708.

**Reaction of (1,1-Dimethyl-2,5-diphenyl-1-silacyclohexadienyl)lithium (10) with $CD_2Cl_2$ in the Presence of BuLi.** In a 50-mL two-necked round-bottomed flask equipped with a magnetic stirring bar, a reflux condenser, and a dropping funnel was placed **9** (313 mg, 1.13 mmol) in ether (20 mL) under an argon atmosphere. To the stirred solution was added 3.8 mL of 1.2 N BuLi in ether (4.6 mmol, 4.0 equiv) dropwise at 0 °C over 10 min. Then the solution was cooled to −78 °C. Dry $CD_2Cl_2$ (302 mg, 3.47 mmol, 3.1 equiv) in ether (1 mL) was added to the anion solution, which was warmed to room temperature gradually. The reaction mixture was hydrolyzed and extracted with ether. After evaporation of the solvent in vacuo, the $^1$H NMR spectrum of the residue showed signals due to the deuterated **11** and **12** as the main products. Then the residue was subjected to TLC on silica gel to give a mixture of 7-deuterio-1,1-dimethyl-2,5-diphenylsilepin (**25**), 5-deuterio-2,2-dimethyl-3,7-diphenyl-2-silabicyclo[3.2.0]hepta-3,6-diene (**26**), and 6-deuterio-2,2-dimethyl-3,7-diphenyl-2-silabicyclo[3.2.0]hepta-3,6-diene (**27**) (839.2 mg, 0.135 mmol, 12%). The ratio of **25** to the mixture of **26** and **27** was estimated to be ca. 1:1 by means of $^1$H NMR spectroscopy. These isomers were separated into **25** (9.1 mg, 0.031 mmol, 2.7%) and a mixture of **26** and **27**, which was estimated to be ca. 9:1 by means of $^1$H NMR spectroscopy. **25**: colorless oil; $^1$H NMR ($CDCl_3$) $\delta$ 0.18 (s, 6 H, SiMe), 6.84 (dd, 1 H, $J_{3,4} = 7.0$ Hz, $J = 1.0$ Hz, H-3 or H-4), 6.91 (d, 1 H, $J_{3,4} = 7.0$ Hz, H-3 or H-4), 7.11 (d, $J = 1.0$ Hz, H-6), 7.2–7.6 (m, 10 H, Ph); $^2$H NMR ($CHCl_3$, internal standard $CDCl_3$ $\delta$ 7.26) $\delta$ 6.10 (D-7); MS $m/z$ (%) 289 ($M^+$, 20), 274 (55), 231 (100), 58 (21); high-resolution MS found 289.1379, calcd for $C_{20}H_{19}DSi$ 289.1398. **26** and **27**: colorless oil; MS $m/z$ (%) 289 ($M^+$, 42), 274 (100), 231 (37), 58 (39); high-resolution MS found 289.1395, calcd for $C_{20}H_{19}DSi$ 289.1398. **26**: $^1$H NMR ($CDCl_3$) $\delta$ 0.09 (s, 3 H, SiMe), 0.42 (s, 3 H, SiMe), 2.91 (br s, 1 H, H-1), 6.55 (br s, 1 H, H-6), 7.03 (s, 1 H, H-4), 7.2–7.5 (m, 10 H, Ph); $^2$H NMR ($CHCl_3$, internal standard $CDCl_3$ $\delta$ 7.26) $\delta$ 4.05 (D-5). **27**: $^1$H NMR ($CDCl_3$) $\delta$ 0.09 (s, 3 H, SiMe), 0.42 (s, 3 H, SiMe), 2.91 (d, 1 H, $J_{1,5} = 3.8$ Hz, H-1), 3.93 (dd, $J_{1,5} = 3.8$ Hz, $J_{4,5} = 3.2$ Hz, H-4), 7.03 (d, 1 H, $J_{4,5} = 3.2$ Hz, H-4), 7.2–7.5 (m, 10 H, Ph); $^2$H NMR ($CHCl_3$, internal standard $\delta$ 7.26) $\delta$ 6.68 (D-4).

# Structural Evidence for Ligand Backbonding in Distortions from Octahedral Geometry of Complexes of $d^6$ $ML_4$ Fragments with $\pi$-Ligands

Donald J. Wink

*Department of Chemistry, New York University, New York, New York 10003*

*Received June 27, 1990*

Variations in the structure of the $ML_4$ portion of $d^6$ $ML_4$($\pi$-ligand) complexes are explored through a survey of structures in the literature and qualitative molecular orbital theory, supported by calculations at the extended Hückel level. The $\pi$-ligands considered are allyl anion, nonconjugated diene, conjugated diene, and alkyne. There are systematic distortions from octahedral geometry in the $ML_4$ fragment, characterized by a bending back of the axial ligands from the $\pi$-ligand and an opening up of the angle for the equatorial ligands. Little bendback of the axial ligands occurs for allyl anion and nonconjugated diene complexes, where $\pi$-backbonding is a modest component of the metal–$\pi$-ligand bonding. A much larger bending back occurs when the $\pi$-ligand is a conjugated diene or an alkyne. These ligands have low-lying $\pi^*$ orbitals and are excellent $\pi$-acids, which stabilizes the distortion through a stronger metal-to-ligand backbond. Equatorial distortion is influenced by steric effects. The equatorial ligands are opened up to an angle greater than 100° in most of the allyl anion, 1,3-diene, and alkyne complexes, but not with the nonconjugated complexes. This is because substituents on the nonconjugated diene ligand only are pointed toward the equatorial sites, preventing the opening up of the equatorial angle. A relationship between a significant ground-state distortion and a low barrier for formal rotation of the $\pi$-ligand is discussed in terms of the ability of the $\pi$ orbitals on the metal to switch roles when the ligand is a good $\pi$-acceptor, as detected in changes in fragment orbital populations. The structures of certain other complexes, with chelation among the $ML_4$ set or with more symmetric $\pi$-ligands (cyclobutadiene, trimethylenemethane, dienyl cation), are shown to be consistent with the trends observed.

## Introduction

Backbonding, where d-electron density is transferred from a transition metal to an unoccupied ligand orbital, is an important part of many metal–ligand interactions. This is especially true with unsaturated organic ligands, and backbonding is a key element of the Dewar–Chatt–Duncanson model of the metal–olefin bond.[1] There have been several structural studies of the influence of backbonding on *ligand* bond lengths, angles, and bond strengths.[2] This was critical, for example, to the evidence advanced by Chatt and Duncanson to support partial occupation of the C–C $\pi^*$-bond in platinum olefin complexes.[1b]

The historical emphasis on the effect of backbonding on a ligand's structure neglects the effect the same interaction must, ispo facto, have on the metal fragment. Just as an olefin, for example, undergoes pyramidalization

(1) (a) Dewar, M. J. S.; Ford, G. P. *J. Am. Chem. Soc.* **1979**, *101*, 783. (b) Chatt, J.; Duncanson, L. A. *J. Chem. Soc.* **1953**, 2339.

(2) (a) Collman, J. P.; Hegedus, L. S.; Norton, J. R.; Finke, R. G. *Principles and Applications of Organotransitionmetal Chemistry*, 2nd ed.; University Science: Mill Valley, CA, 1987. (b) Elschenbroich, C.; Salzer, A. *Organometallics*; Verlag-Chemie: New York, 1989.

0276-7333/91/2310-0442$02.50/0 

to maximize the overlap of its vacant orbital with a metal, so the metal and its other ligands may distort to make the filled orbital that will backbond to the ligand *more accessible to the ligand*. Such effects have been noted in extremely broad or dramatic cases before. The seminal work of Hoffmann and co-workers included mention,[3,4] for example, of the distortion of a $d^6$ $ML_4$ fragment from a pseudooctahedral $C_{2v}$ geometry with a simple nonconjugated diene ligand toward a pyramidal $C_{4v}$ structure with cyclobutadiene. This was explained in terms of the nondegenerate $\pi$-donor/$\pi$-acceptor set of orbitals on the diene in a simple diene and a degenerate set in cyclobutadiene.

But there is no need to restrict even qualitative discussions to only dramatic changes in molecular structure and bonding. More subtle changes are appropriate for study when the changes are clearly systematic. This paper reports such a study on the effects of $\pi$-bonding on the metal fragment structure in $d^6$ $ML_4$ complexes of $\pi$-ligands capable of donating four electrons to the metal. The most relevant $\pi$-ligands are allyl anion, nonconjugated diene, conjugated diene, and alkyne. For the $L_4$ set, any monodendate two-electron donor ligands are accepted. Other systems with more symmetric $\pi$-ligands (cyclobutadiene, trimethylenemethane, and dienyl cation) or with chelate ligands within the $L_4$ set are considered secondarily.

The effects we observe and explain are large, and variations among the $L_4$ set are not significant. Of course, a large enough data set could serve as a basis for the systematic study of the effect of various ligands in the L set. But there are not enough structures in the literature in this case for such a study. A fine example of this in a much larger data set is provided by Poli in his discussion of "piano-stool" complexes, $ML_4$(cyclic $\pi$-ligand).[5]

## Results and Discussion

**Geometry of the $ML_4$ Fragment and Literature Survey.** The $ML_4$ fragment is formed by the removal of two cis ligands from an octahedron. The fragment has $C_{2v}$ symmetry with two ligands in axial sites and two in equatorial sites. The angles about the metal are defined by one for the axial ligands ($\phi$) and one for the equatorial ligands ($\theta$), as in **1**. A structure derived directly from an

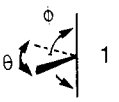

1

octahedron would have $\phi = 180°$ and $\theta = 90°$. There are two distortions that occur when this fragment forms a complex with a $\pi$-ligand. The two equatorial ligands can swing forward through an increase in $\theta$ (**2**), and the axial ligands can swing back with a decrease in $\phi$ (**3**).

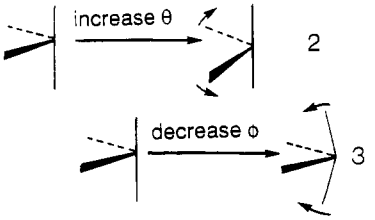

2 3

The structures that meet the definition required for this study are listed in Table I with unambiguous nomenclature or by a reference to a PLUTO drawing in Figure 1. The $\theta$ and $\phi$ values for the complexes are taken from the literature or calculated from atomic coordinates (as indicated by the absence of an estimated standard deviation (esd)). The structures are grouped according to the type of unsaturated ligand involved, $\eta^3$-allyl anion,[6] nonconjugated diene,[7] conjugated diene,[6f,8] and alkyne,[9] and within each

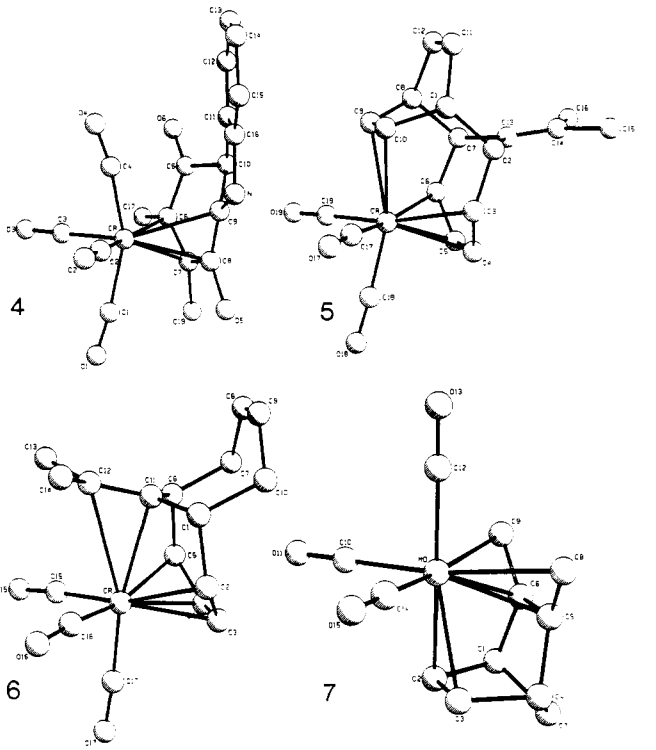
4 5 6 7

**Figure 1.** PLUTO drawings of the core structures for complexes with complicated $\pi$-ligands, provided for clarity.

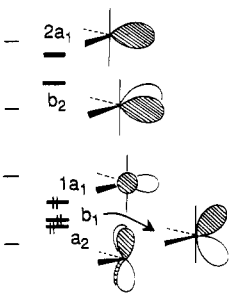


**Figure 2.** Frontier molecular orbitals for the $d^6$ $ML_4$ fragment, with energies calculated for $Cr(CO)_4$ at $\phi = 180°$, $\theta = 90°$.

(3) Elian, M.; Hoffmann, R. *Inorg. Chem.* **1975**, *14*, 1058.
(4) Albright, T. A.; Hoffmann, R.; Tse, Y.; D'Ottavio, T. *J. Am. Chem. Soc.* **1979**, *101*, 3812.
(5) Poli, R. *Organometallics* **1990**, *9*, 1892.

(6) (a) Tulip, T. H.; Ibers, J. A. *J. Am. Chem. Soc.* **1979**, *101*, 4201. (b) Kaduk, J. A.; Poulos, A. T.; Ibers, J. A. *J. Organomet. Chem.* **1977**, *127*, 245. (c) Hewitt, T. G.; deBoer, J. J.; Anzenhofer, K. *Acta Crystallogr.* **1970**, *26B*, 1244. (d) Simon, F. E.; Lauher, J. W. *Inorg. Chem.* **1980**, *19*, 2338. (e) Paz-Sandoval, M. A.; Powell, P.; Drew, M. G. B.; Perutz, R. N. *Organometallics* **1984**, *3*, 1026. (f) Wang, N.-F.; Wink, D. J.; Dewan, J. C. *Organometallics* **1990**, *9*, 335. (g) Bassi, J. W.; Scordamaglia, R. *J. Organomet. Chem.* **1973**, *51*, 273. (h) Wink, D. J.; Wang, N.-F.; Springer, J. P. *Organometallics* **1989**, *8*, 259. (i) Merola, J. S. *Organometallics* **1989**, *8*, 2975.
(7) (a) Grevels, F.-W.; Jacke, J.; Betz, P.; Krüger, C.; Tsay, Y.-H. *Organometallics* **1989**, *8*, 293. (b) Huttner, G.; Mills, O. S. *J. Organomet. Chem.* **1971**, *29*, 275. (c) Oosthuizen, H. E.; Singleton, E.; Field, J. S.; van Niekerk, G. C. *J. Organomet. Chem.* **1985**, *279*, 433. (d) Gould, R. O.; Jones, C. L.; Robertson, D. R.; Stephenson, T. A. *J. Chem. Soc., Dalton Trans.* **1977**, 129. (e) Declercq, J. P.; Germain, G.; van Meerssche, M.; Chaudhury, S. A. *Acta Crystallogr.* **1975**, *31B*, 2896. (f) Wink, D. J.; Wang, N.-F.; Creagan, B. T. *Organometallics* **1989**, *8*, 561. (g) Wink, D. J.; Oh, C. K. *Organometallics* **1990**, *9*, 2403. (h) Potvin, C.; Manoli, J. M.; Pannetier, G.; Chevalier, R. *J. Organomet. Chem.* **1978**, *146*, 57.
(8) (a) Kreiter, C. G.; Kotzian, M.; Schubert, U.; Bau, R.; Bruck, M. *Z. Naturforsch.* **1984**, *39B*, 1553. (b) Pavkovic, S. F.; Zaluzec, E. J. *Acta Crystallogr.* **1989**, *45C*, 18.

**Table I. Complexes for Primary Study**

| complex | θ, deg | φ, deg | ref |
|---|---|---|---|
| $\eta^3$-Allyl Complexes | | | |
| $IrHCl(PPh_3)_2(\eta^3$-(*E*)-phenyl-2-propen-1-yl) | 101.6 (1) | 176.0 (3) | 6a |
| $Ir(CO)Cl(PPhMe_2)_2(\eta^3$-2-propen-1-yl) | 105.7 (1) | 176.0 (4) | 6b |
| $RhCl_2(AsPh_3)_2(\eta^3$-2-methyl-2-propen-1-yl) | 106.25 (6) | 174.0 (1) | 6c |
| *fac*-$Fe(CO)_3Br(\eta^3$-2-propen-1-yl) | 105.9 (4) | 171.9 (4) | 6d |
| *fac*-$Mn(PMe_3)(CO)_3(\eta^3$-(*Z*)-penta-2,4-dien-1-yl) | 99.5 (5) | 170.8 (3) | 6e |
| [*fac*-$Cr(P(OMe)_3)(CO)_3(\eta^3$-(*Z*)-2-buten-1-yl)]$^-$ | 95.6 (2) | 170.8 (1) | 6f |
| $Mo(CO)_4$(triphenyl($\eta^3$-2-propen-1-yl)-phosphine | 91.4 (3) | 168 (1) | 6g |
| [*fac*-$Cr(P(OMe)_3)(CO)_3(\eta^3$-(*E*)-2-methyl-2-buten-1-yl)]$^-$ | 101.4 (3) | 167.8 (2) | 6h |
| [$Ir(PMe_3)_3(C_6H_5)(\eta^3$-(*E*)-2-buten-1-yl)]$^+$ | 104.2 (2) | 163.3 (1) | 6i |
| average | 101 (5) | 171 (4) | |
| $\eta^4$-Nonconjugated Dienes | | | |
| *mer*-$W(CO)_3(\eta^2$-$C_2H_4)(\eta^4$-bicyclo-[2.2.1]heptadiene) | 91.7 | 171.6 (3) | 7a |
| $Cr(CO)_4(\eta^4$-hexamethylbicyclo[2.2.0]-hexa-2,5-diene) | 92.1 (9) | 168.6 (8) | 7b |
| $W(CO)_4(\eta^4$-bicyclo[2.2.1]heptadiene) | 94.3 (2) | 167.6 (2) | 7a |
| $Os(CNBu^t)_2(NH_2NCMe_2)_2(\eta^4$-1,5-cyclooctadiene) | 93 (1) | 167 (1) | 7c |
| $Ru(CO)(NCMe)Cl_2(\eta^4$-1,5-cyclo-octadiene) | 92.6 (2) | 166.6 (9) | 7d |
| *mer*-$Cr(CO)_3(PPh_3)(\eta^4$-bicyclo[2.2.1]-heptadiene) | 101.5 (3) | 166.2 (4) | 7e |
| *mer*-$Cr(CO)_3P(OMe)_3(\eta^4$-1,5-cyclo-octadiene) | 96.3 (2) | 165.5 (3) | 7f |
| *fac*-$W(CO)_3P(OMe)_3(\eta^4$-1,5-cyclo-octadiene) | 95.9 (2) | 163.8 (2) | 7g |
| $RuHCl(piperidene)_2(\eta^4$-1,5-cyclo-octadiene) | 86.52 (8) | 161 (1) | 7h |
| average | 94 (4) | 166 (3) | |
| $\eta^4$-Conjugated Dienes | | | |
| $Cr(CO)_2(PMe_3)_2(\eta^4$-1,3-pentadiene) | 112 (2) | 159.7 (2) | 8a |
| *fac*-$Cr(CO)_3(P(OMe)_3)(\eta^4$-1,3-butadiene) | 103.2 (2) | 158.2 (2) | 6f |
| 4 | 100.9 (2) | 155.4 (2) | 8b |
| $Cr(CO)_2(PMe_3)_2(\eta^4$-2,4-hexadiene) | 101.8 (8) | 151.6 (2) | 8a |
| average | 104 (4) | 154 (3) | |
| $\eta^2$-Alkyne | | | |
| $Cr(CO)_2(P(OMe)_3)_2(\eta^2$-PhC≡CPh) | 107.0 (3) | 153.94 (7) | 9 |

group the complexes are listed in order of decreasing φ. The different π-ligands are extraordinarily predictive of the structure of the $ML_4$ fragment. There is some overlap in the φ values for the allyl (φ = 176.0–163.3°) and nonconjugated diene complexes (φ = 171.6–161°) while the conjugated diene (φ = 159.7–151.6°) and alkyne structures (φ = 153.9°) form a distinct set. The variations in θ within a set are generally much larger than in φ, but it is still easy to see that significant increases in θ occur with the allyl anion, 1,3-diene, and alkyne ligands while there is very little increase in θ for complexes with nonconjugated diene ligands.[7] There are also several complexes related to the primary set, but which are excluded because they contain chelating groups,[10,11] a highly symmetric π-ligand,[12] highly unusual electronic requirements,[6d] or intermolecular contacts.[13] Their relevant structural parameters are given in Table II.

**Table II. Exceptional Complexes**

| complex | θ, deg | φ, deg | ref |
|---|---|---|---|
| Chelate-Containing Systems | | | |
| $Mn(PMe_2CH_2CH_2PMe_2)_2(\eta^3$-(*E*)-pentadienyl) | 99.3 (2) | 169.3 (3) | 10 |
| 5 | 102.2 (2) | 155.5 (3) | 11a |
| 6 | 92.8 (2) | 173.9 (3) | 11b |
| 7 | 89.4 (1) | 165.0 | 11c |
| Extended π-Ligands | | | |
| $Cr(CO)_3(PPh_3)(\eta^4$-trimethylene-methane) | 121.1 (5) | 140.8 (4) | 12a |
| $Cr(CO)_3(PPh_3)(\eta^4$-benzocyclo-butadiene) | 112.4 (1) | 149.7 (2) | 12b |
| $Mo(CO)_3(PPh_3)(\eta^4$-cyclobutadiene) | 111.0 | 146.6 | 12c |
| $Mo(CO)_3(PPh_3)(\eta^4$-cyclobutadiene) | 110.1 | 138.8 | 12c |
| $Mn(CO)_2(dppe)(\eta^5$-$C_5H_7)$ | 109.9 (1) | 141.7 (1) | 12d |
| System with Intrmolecular Contact in the Solid State | | | |
| $RuCl_2(NH_2Ph)_2$(bicyclo[2.2.1]heptadiene) | 93.7 (1) | 156.5 (5) | 13 |
| System with Unusual Electronic Requirements | | | |
| *mer*-$Fe(CO)_3(AuPPh_3)(\eta^3$-2-propen-1-yl) | 106.3 (3) | 142.9 (3) | 6d |

The $ML_4$ fragment derived from the octahedron has a frontier orbital structure as depicted in Figure 2.[3,14] Only one of the filled predominantly d orbitals, of $b_1$ symmetry and derived from the metal $d_{xz}$ orbital, is oriented to backbond to a ligand in the vacant site. The others, $a_2$ and $1a_1$, are more localized in bonding to the $L_4$ set. These have a minimal effect either on the energy of the fragment or on the bonding to the π-ligand. Therefore, they will be omitted from subsequent discussion and illustrations. There are, finally, two vacant orbitals on the metal fragment that are at relatively low energy. These orbitals, $b_2$ and $2a_1$, are oriented to accept electron density from the vacant coordination site.

The energy, size, and shape of the frontier orbitals are affected by distortions from a true octahedral relationship. The opening up of the equatorial angle θ, **2**, has a minimal effect on the total energy of the $ML_4$ fragment. The only significant effect of this motion is on one of the vacant orbitals: there is a significant drop in the energy of the fragment LUMO, $b_2$, as θ is increased. Lowering the energy of the metal fragment $b_2$ orbital will decrease the gap between it and the ligand $b_2$ donor orbital, strengthening the $b_2$ ligand-to-metal donor interaction.

The effect of bending back of the axial ligands, **3**, is much more dramatic. The filled $b_1$ orbital ($d_{xz}$) of the fragment rises significantly in energy and even becomes the fragment HOMO when φ is 160°. The distortion is accompanied by a mixing in of $p_z$ character into the orbital; this decreases the backbonding to the axial ligands, and the $b_1$ orbital becomes *more strongly oriented toward the vacant site.* Finally, both of the unoccupied orbitals on the fragment rise in energy as the axial ligands are bent back, especially the σ-acceptor orbital $2a_1$.

The effects of these changes mean that the distortions of the $ML_4$ fragment are in themselves energetically unfavorable (there is a calculated increase in energy for the fragment of about 12 kcal $mol^{-1}$ in going to φ = 160°, θ = 106°). Thus, there must be some especially favorable interaction in the metal–π-ligand bonding to stabilize the

(9) Wink, D. J.; Creagan, B. T. *J. Am. Chem. Soc.* **1990**, *112*, 8585.
(10) Bleeke, J. R.; Kotyk, J. J. *Organometallics* **1985**, *4*, 194.
(11) (a) Michels, E.; Sheldrick, W. S.; Kreiter, C. G. *Chem. Ber.* **1985**, *118*, 964. (b) Kreiter, C. G.; Michels, E.; Kaub, J. *Z. Naturforsch.* **1986**, *41B*, 722. (c) Anderson, B. F.; Robertson, G. B.; Butler, D. N. *Can. J. Chem.* **1976**, *54*, 1958.
(12) (a) Henslee, W. E.; Davis, R. E. *J. Organomet. Chem.* **1974**, *81*, 389. (b) Oliver, J. Ph.D. Thesis, The University of Texas at Austin, 1971. (c) Davis, R. E. Personal communication. (d) Lee, G. H.; Peng, S. M.; Tsung, I. C.; Mu, D.; Liu, R.-S. *Organometallics* **1989**, *8*, 2248.
(13) Manoli, J.-M.; Gaughan, A. P., Jr.; Ibers, J. A. *J. Organomet. Chem.* **1974**, *72*, 247.
(14) (a) Albright, T. A.; Burdett, J. K.; Whangbo, M.-H. *Orbital Interactions in Chemistry*; Wiley-Interscience: New York, 1985. (b) Burdett, J. *Molecular Shapes*; Wiley: New York, 1980.

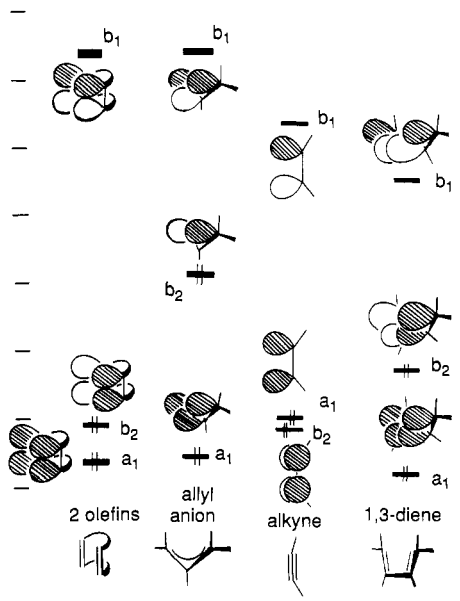


**Figure 3.** Frontier molecular orbitals for the $\pi$-ligands in the study.

distortion. This can be either a superior $\pi$-donor interaction, to take advantage of the drop in the fragment $b_2$ orbital as $\theta$ increases, or a good $\pi$-acceptor interaction, to take advantage of the rise in energy of the $b_1$ orbital as $\phi$ decreases, or both.

**Ligand Orbitals.** The ligands in the primary portion of this study (Table I) all possess three orbitals of the energy and shape appropriate for interaction with the metal (we will neglect $\delta$-symmetry interactions). These are presented, on a common energy scale, in Figure 3. They can be classed according to the symmetry of the metal orbital that they will interact with.[15] Two ligand orbitals interact with the vacant $a_1$ and $b_2$ orbitals of the $ML_4$ fragment in $\sigma$- and $\pi$-donor fashion. The LUMO of the $\pi$-ligand functions as a $\pi$-acceptor orbital with the filled metal $b_1$ orbital; this ligand LUMO varies significantly in energy among the four ligands. For the allyl anion, the LUMO is antibonding between the central carbon and both terminal carbons. With two nonconjugated olefins, it also represents two pure C–C $\pi^*$-interactions, though these may be *slightly* moderated by pyramidalization. The severe bending back of the substituents on an alkyne makes the LUMO less antibonding because the overlap of the $\pi$ orbitals decreases considerably, so this orbital drops significantly in energy. With the 1,3-diene, finally, the LUMO is bonding between the central two carbons and, while the interaction across the whole system is still antiboding, the orbital is significantly stabilized by the conjugation with respect to two isolated $\pi^*$ orbitals.

**Calculated Molecular Structures and Distortions from Octahedral Geometry.** The interaction diagram for the $ML_4$ fragment with the three important orbitals of the $\pi$-ligands is given schematically in Figure 4 (note that, for clarity, the $1a_1$ orbital and $a_2$ orbital of the $ML_4$ are omitted). Certain important parameters that are associated with complexes of each of the four ligands are given in Table III. In all cases, in accord with the prediction of Elian and Hoffmann,[3] the energy surface for distortion is "rather soft". But it is nonetheless quite definitive and indicates well the nature of the major interactions. The most stable structures for the allyl anion and the nonconjugated diene case are quite close to octahedral while those for the 1,3-diene and the alkyne are more distorted. This nicely matches the experimental trend.

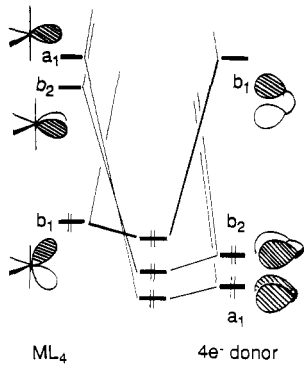


**Figure 4.** Schematic interaction diagram for the ideal orientation for the $\pi$-ligands.

**Table III. Calculated Parameters for the Minimum Energy Geometry for Each Ligand[15]**

| | allyl anion | two olefins | 1,3-diene | alkyne |
|---|---|---|---|---|
| Characteristics of Minimum Energy Structure | | | | |
| energy stabilization[a,b] | 3 | 1 | 15 | 5 |
| $\theta$, deg | 98 | 90 | 106 | 106 |
| $\phi$, deg | 170 | 170 | 160 | 160 |
| Population of Key Orbitals at Minimum Energy Structure | | | | |
| $ML_4$ $b_1$ | 1.96 | 1.78 | 1.63 | 1.48 |
| $ML_4$ $b_2$ | 0.66 | 0.36 | 0.46 | 0.31 |
| ligand "$b_2$" | 1.32 | 1.64 | 1.55 | 1.63 |
| ligand "$b_1$" | 0.11 | 0.24 | 0.47 | 0.57 |
| Other Parameters | | | | |
| overlap of "$b_1$" orbitals | 0.10 | 0.17 | 0.14 | 0.28 |
| rotational barrier[a] | 60 | >140 | 32 | 18 |

[a] In kcal mol$^{-1}$. [b] Relative to $\theta = 90°$, $\phi = 180°$.

The relationship of the $\pi$-backbonding interaction to the bending back of the axial ligands is immediately apparent when one looks at changes in orbital population when a complex is formed. The occupancy of the ligand LUMO increases and the occupancy of the $ML_4$ $b_1$ orbital decreases monotonically from the allyl anion to the alkyne, indicating a gradual increase in the extent of $\pi$-backbonding. The LUMO's of the conjugated diene and the alkyne in particular are quite low in energy and interact very strongly with the metal $b_1$; these are very good $\pi$-acceptor ligands, far superior to the nonconjugated diene and allyl anion.

The alkyne and the 1,3-diene ligand differ in their $\pi$-acceptor capabilities for two reasons. The LUMO of a 1,3-diene ligand lies at lower energy than that for an alkyne (Figure 3); it should be a better $\pi$-acceptor. But the overlap integral for the relevant fragment orbitals is also important (Table III). The overlap for the alkyne is by far the largest, because the alkyne $b_1$ orbital is coplanar with the metal $b_1$. The net effect is that the alkyne is better as a $\pi$-acceptor than the 1,3-diene even though the alkyne LUMO lies at higher energy than the 1,3-diene LUMO.

It is important to note that the bending back of the axial ligands is apparently *not* influenced by steric factors. We have already documented in our own work how close contacts between the ligands in *fac*-$W(CO)_3(P(OMe)_3)(\eta^4$-1,5-COD)[7g] and [*fac*-$Cr(CO)_3(P(OMe)_3)(\eta^3$-allyl)]$^-$ [6f,h] complexes imply that these complexes are quite crowded, and yet the bending back is modest in all cases.

(15) For the allyl anion and conjugated diene, the molecular symmetry will only be $C_s$, but we have chosen to stay with the $C_{2v}$ labels for the sake of consistency; there is little mixing of the orbitals, according to our calculations.

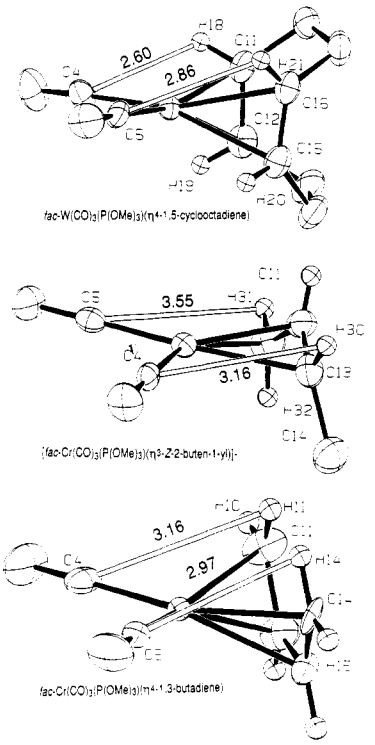


**Figure 5.** ORTEP drawings of the core structures for a representative (a) nonconjugated diene, (b) allyl anion, and (c) conjugated diene structure, indicating the closet contacts between substituents on the $\pi$-ligand and the equatorial groups.

Of course a compromise is reached between electronic and steric factors, but we emphasize that this is much on the electronic side in each case: despite steric crowding, a serve bendback does not occur unless the ligand is a good $\pi$-acceptor.

The experimental data in Table I indicate that there is a modest increase in $\theta$ with complexes of allyl anions, conjugated dienes, and the alkyne. This is because, as noted before, an increase in $\theta$ results in a lowering of the energy of the vacant $b_2$ orbital on the metal and an increase in the ligand-to-metal $\pi$-donor interaction. This is favored with these $\pi$-ligands, which are all good $\pi$-donors. Calculations also predict that an increase in $\theta$ is favored for the nonconjugated dienes. However, the values observed experimentally are much less than for the other three $\pi$-ligands. This is because of steric effects that are most pronounced with the nonconjguated dienes. Increases in $\theta$ will eventually cause crowding between the equatorial ligands and the $\pi$-ligand. Figure 5 presents details of the cores of three structures, all derived from *fac*-$M(CO)_3(P(OMe)_3)(\pi$-ligand) complexes. With both the allyl anion and the butadiene, the substituents on the $\pi$-ligands are far away from the equatorial ligands, despite a significant increase in $\theta$ from 90°. With the cyclooctadiene complex, on the other hand, the hydrogens on the ligands are necessarily pointed *toward* the metal—and the cis ligands. Much closer contacts are seen, and the increase in $\theta$ is small.

**Relationship between Ground-State Geometry and Intramolecular Rearrangements.** The variation in $\pi$-acceptor capability of the $\pi$-ligands will also affect the barrier for simple rotation of the $\pi$-ligand. Complexes with 1,3-dienes or an alkyne have very low (<30 and <15 kcal $mol^{-1}$) rotational barriers[9,16] while complexes with nonconjugated dienes and the allyl anions are quite rigid.[17]

(16) Kreiter, C. G. *Adv. Organomet. Chem.* **1986**, *26*, 297.

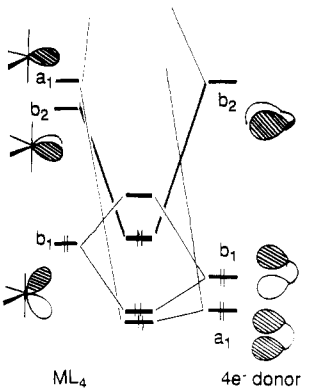


**Figure 6.** Schematic interaction diagram for the orientation for the $\pi$-ligands 90° from the ideal, indicating the "inverted role" of the HOMO and LUMO orbitals of the ligand.

This can be partly explained by letting the distortions go even further, toward a square pyramid, as is suggested in the case of simple olefin rotation in $Fe(CO)_4(C_2H_4)$ complexes.[18] But in fact a further distortion of the $ML_4$ fragment is not required with a ligand that is *both* a good $\pi$-acceptor and good $\pi$-donor. Our calculations show that, at the ground-state structure for each type of ligand, there are rather low barriers for simple rotation of the alkyne (18 kcal $mol^{-1}$) and 1,3-diene (32 kcal $mol^{-1}$) and very large barriers (>50 kcal $mol^{-1}$) for both the nonconjugated diene and the allyl anion. This suggests a more interesting effect to explain the low barrier with alkynes and 1,3-dienes, concerning the unique relationship of the $\pi$-donor and $\pi$-acceptor orbitals of the diene and alkyne ligands.

While the effective $\sigma$-donor interaction, $a_1$, is, to a first approximation, symmetric with respect to the metal–ligand axis, both the $\pi$-donor $b_2$ and $\pi$-acceptor $b_1$ interactions are asymmetric. Either $\pi$-interaction, *alone*, will strongly suppress simple rotation of the $\pi$-ligand. However, these orbitals are also *orthogonal to one another and, in an alkyne or a conjugated diene, relatively close in energy.* This enables the HOMO and LUMO of the metal fragment in the alkyne and the conjugated diene complexes to *invert their roles* when the ligand is rotated by 90°.

The ground-state interaction, as sketched in Figure 4, includes a conventional backbonding orbital, **8**, between a filled orbital on the metal and an unfilled orbital on the ligand. When the ligand is rotated by 90°, this interaction

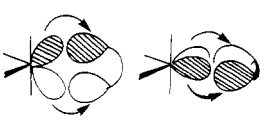

**8** **9**

will be lost and, moreover, a filled–filled conflict will result between the ligand and the metal $b_1$ orbitals. However, if the ligand is a good $\pi$-acceptor, then the formally vacant orbitals on the metal and the ligand combine to form an orbital that will be low enough in energy to be the molecular HOMO, as sketched in Figure 6. As we discussed in a treatment of alkyne rotation in polyalkyne complexes,[19] a potential antibonding interaction between two filled orbitals is "avoided" by an excellent $\pi$-backbond formed by the LUMO of the $ML_4$ and the $\pi$-ligand, which then

(17) (a) Faller, J. W.; Adams, M. A. *J. Organomet. Chem.* **1979**, *170*, 71. (b) Palmer, G. T.; Basolo, F. *J. Am. Chem. Soc.* **1985**, *107*, 3122.
(18) Albright, T. A.; Hoffmann, R.; Thibeault, J. C.; Thorn, D. L. *J. Am. Chem. Soc.* **1979**, *101*, 3801.
(19) Wink, D. J.; Creagan, B. T. *Organometallics* **1990**, *9*, 328.

**Table IV. Parameters for Extended Hückel Calculations**

| orbital | | $H_{ij}$, eV | $\zeta_1$ | $\zeta_2$ | $C_1$ | $C_2$ |
|---|---|---|---|---|---|---|
| Cr | 3d | −11.22 | 4.95 | 1.60 | 0.4876 | 0.7205 |
| | 4s | −8.66 | 1.70 | | | |
| | 4p | −5.24 | 1.70 | | | |
| C | 2s | −21.40 | 1.625 | | | |
| | 2p | −11.40 | 1.625 | | | |
| O | 2s | −32.30 | 2.275 | | | |
| | 2p | −14.80 | 2.275 | | | |
| H | 1s | −13.60 | 1.30 | | | |

form the HOMO of the molecule, as in **9**.

**Exceptional Complexes.** There are four types of compounds listed in Table II that, though they meet the definition of a $\pi$-complex of a $d^6$ $ML_4$ fragment, are best treated separately. Chelated systems may or may not experience constraints in ligand angles based on the chelate ring. The case of a 1,2-bis(dimethylphosphinoethane (dmpe) manganese complex,[10] for example, shows that the values of $\theta$ and $\phi$ that are associated with an allyl anion system hold here too, but in fact that chelate ring system does exhibit rapid fluxional behavior, an exception to normal cases. The three cases with a triene ligand are related to each other. Two, **6**[11b] and **7**,[11c] are particularly rigid and it is not surprising that the chelate ring prevents the axial ligand from swinging away to a position with small $\phi$. In the one case where the hydrocarbon ring is larger, **5**,[11a] a more normal value of $\phi$ is found.

Systems with extended $\pi$-ligands based on more than four carbon atoms or with more symmetric $\pi$-systems such as cyclobutadiene have been discussed theoretically by several other groups.[4,5,20] These ligands have even smaller splittings between the formally $\pi$-donor and $\pi$-acceptor orbitals (in cyclobutadiene there is a degeneracy). Following arguments made above, larger distortions in complexes of these ligands are expected and, indeed, are found (Table II).

The final two exceptional cases[10d,13] do not fit the experimental trend at all. This is easily explained either because an intermolecular contact in the solid state (a hydrogen bond) may distort the structure or because the unusual electronic requirements of one of the ligands (a gold complex) make the formal assignment of a $d^6$ metal center dubious.

## Conclusion

The literature survey presented here shows that ligands can induce regular distortions in a metal fragment. This is very important because the fragment structure can have profound effects on spectroscopy and reactivity, and it is imperative that even small structural changes be considered in any explanation of the reactivity of this metal–ligand environment. For example, group 6 $ML_4$($\pi$-ligand) complexes are important in the catalysis of diene hydrogenation.[7a,21] The present results suggest that any study of the chemistry of that system must pay careful attention to the influence of ligand type on structure and reactivity.

There are certainly many other examples in the literature of nominally "soft" potential surfaces that, under the influence of a set of ligands, become much more rigid and regular. This should enable observant structural and theoretical chemists to develop clearer rules for the nature and degree of the influence of ligands on metal fragment structure, perhaps driving certain synthetic programs that seek to exploit—or thwart—such rules.

**Acknowledgment.** We thank the donors of the Petroleum Research Fund, administered by the American Chemical Society, for financial support.

## Appendix

All quantitative data were obtained from calculations performed by using the extended Hückel method with the modified Wolfgang–Helmholtz procedure.[22] Parameters, taken from Albright et al.,[23] are listed in Table IV. The C–O bond distance was fixed at 1.20 Å and the Cr–C(O) distance at 1.80 Å. The alkyne geometries were set with a C–C bond of 1.30 Å and a C–C–H angle of 155°; a fixed distance of 1.95 Å from the Cr to the alkyne carbons was used. The allyl anion geometry was set with a C–C bond length of 1.38 Å and a distance from the Cr to the central and terminal carbons of 2.16 and 2.24 Å, respectively. The butadiene geometry was set with C–C bond distances of 1.42 and 1.38 Å for the internal and terminal bonds and Cr–C distances of 2.15 and 2.25 Å to the internal and terminal positions, respectively. The nonconjugated diene complex was modeled with two separate cis parallel ethylene ligands with a Cr–C distance of 2.20 Å.

(20) Albright, T. A.; Hofmann, P.; Hoffmann, R. *J. Am. Chem. Soc.* **1977**, *99*, 7546.

(21) For leading references and a series of comprehensive spectroscopic studies, see: (a) Jackson, S. A.; Hodges, P. M.; Poliakoff, M.; Turner, J. J.; Grevels, F.-W. *J. Am. Chem. Soc.* **1990**, *112*, 1221. (b) Hodges, P. M.; Jackson, S. A.; Jacke, J.; Poliakoff, M.; Turner, J. J.; Grevels, F.-W. *J. Am. Chem. Soc.* **1990**, *112*, 1234.

(22) Ammeter, J. H.; Bürgi, H.-B.; Thibeault, J. C.; Hoffmann, R. *J. Am. Chem. Soc.* **1978**, *100*, 3686.

(23) Albright, T. A.; Hofmann, P.; Hoffmann, R.; Lillya, C. P.; Dobosh, P. A. *J. Am. Chem. Soc.* **1983**, *105*, 3396.